

Solution and Computed Structure of *ortho*-Lithium *N,N*-Diisopropyl-*P,P*-diphenylphosphinic Amide. Unprecedented Li–O–Li–O Self-Assembly of an Aryllithium

Ignacio Fernández,[†] Pascual Oña-Burgos,[†] Josep M. Oliva,[‡] and Fernando López Ortiz^{*†}

Área de Química Orgánica, Universidad de Almería, Crta. Sacramento s/n, 04120, Almería, Spain, and Instituto de Química-Física "Rocasolano", CSIC, Serrano 119, Madrid, Spain

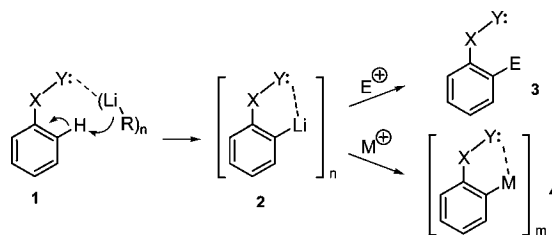
Received December 15, 2009; E-mail: flortiz@ual.es

Abstract: The structural characterization of an *ortho*-lithiated diphenylphosphinic amide is described for the first time. Multinuclear magnetic resonance (¹H, ⁷Li, ¹³C, ³¹P) studies as a function of temperature and concentration employing 1D and 2D methods showed that the anion exists as a mixture of one monomer and two diastereomeric dimers. In the dimers the chiral monomer units are assembled in a *like* and *unlike* manner through oxygen–lithium bonds, leading to fluxional ladder structures. This self-assembling mode leads to the formation of Li₂O₂ four-membered rings, a structural motif unprecedented in aryllithium compounds. DFT computations of representative model compounds of *ortho*-lithiated phosphinic amide monomer and Li₂C₂ and Li₂O₂ dimers with different degrees of solvation by THF molecules showed that Li₂O₂ dimers are thermodynamically favored with respect to the alternative Li₂C₂ structures by 4.3 kcal mol⁻¹ in solvent-free species and by 2.3 kcal mol⁻¹ when each lithium atom is coordinated to one THF molecule. Topological analysis of the electron density distribution revealed that the Li₂O₂ four-membered ring is characterized by four carbon–lithium bond paths and one oxygen–oxygen bond path. The latter divides the Li–O–Li–O ring into two Li–O–Li three-sided rings, giving rise to two ring critical points. On the contrary, the bond path network in the Li₂C₂ core includes a catastrophe point, suggesting that this molecular system can be envisaged as an intermediate in the formation of Li₂O₂ dimers. The computed ¹³C chemical shifts of the C–Li carbons support the existence of monomeric and dimeric species containing only one C–Li bond and are consistent with the existence of tricoordinated lithium atoms in all species in solution.

Introduction

Ortho lithiation assisted by heteroatom-containing functional groups is a powerful synthetic strategy in organic and organometallic chemistry.¹ The functional group facilitates the approach of the lithium base to the deprotonation site and contributes to the stabilization of the *ortho*-lithiated species through intramolecular coordination (Scheme 1).² Subsequent electrophilic trapping provides derivatized aromatic systems **3**

Scheme 1. Directed *Ortho* Lithiation and Trapping Reactions



with very high degrees of regiocontrol.^{1,3} In the organometallic arena, the *ortho*-lithium intermediate represents a valuable

[†] Universidad de Almería.

[‡] Instituto de Química-Física "Rocasolano", CSIC.

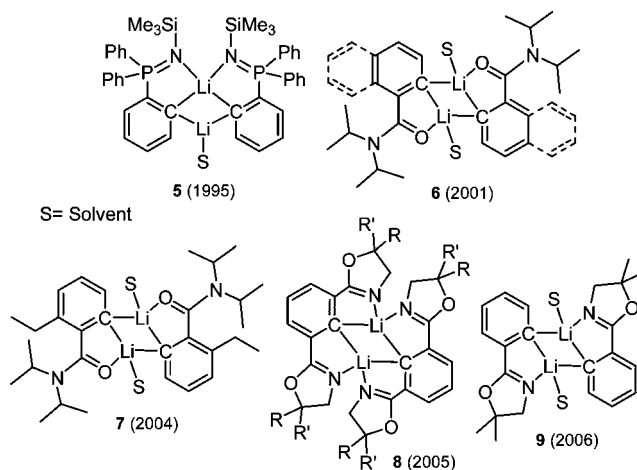
- (1) (a) Clayden, J. *Organolithiums: Selectivity for Synthesis*; Pergamon: Oxford, 2002. (b) Muges, G.; Singh, H. B. *Acc. Chem. Res.* **2002**, *35*, 226. (c) Wheatley, A. E. *Eur. J. Inorg. Chem.* **2003**, 3291. (d) Schlosser, M. *Angew. Chem., Int. Ed.* **2005**, *44*, 376. (e) Chinchilla, R.; Nájera, C.; Yus, M. *Tetrahedron* **2005**, *61*, 3139. (f) Goldfuss, B. *Synthesis* **2005**, 2771. (g) Wu, G.; Huang, M. *Chem. Rev.* **2006**, *106*, 2596.
- (2) For reviews see: (a) Beak, P.; Meyers, A. I. *Acc. Chem. Res.* **1986**, *19*, 356. (b) Beak, P.; Basu, A.; Gallagher, D. J.; Park, Y. S.; Thayumanavan, S. *Acc. Chem. Res.* **1996**, *29*, 552. (c) Basu, A.; Thayumanavan, S. *Angew. Chem., Int. Ed.* **2002**, *41*, 716. (d) Whisler, M. C.; MacNeil, S.; Snieckus, V.; Beak, P. *Angew. Chem., Int. Ed.* **2004**, *43*, 2206. See also: (e) Van Eikema Hommes, N. J. R.; Schleyer, P. V. R. *Angew. Chem., Int. Ed. Engl.* **1992**, *31*, 755. (f) Van Eikema Hommes, N. J. R.; Schleyer, P. V. R. *Tetrahedron* **1994**, *50*, 5903. (g) Kremer, T.; Junge, M.; Schleyer, P. V. R. *Organometallics* **1996**, *15*, 3345.

- (3) (a) Clayden, J. P. In *Patai Series: The Chemistry of Functional Groups. The Chemistry of Organolithium Compounds*; Rappoport, Z., Marek, I., Eds.; Wiley: Chichester, 2004; Part 1, pp 495–646. (b) He, P.; Dong, C.-G.; Hu, Q.-S. *Tetrahedron Lett.* **2008**, *49*, 1906. (c) Coldham, I.; Patel, J. J.; Raimbault, S.; Whittaker, D. T. E.; Adams, H.; Fang, G. Y.; Aggarwal, V. K. *Org. Lett.* **2008**, *10*, 141. (d) O'Brien, P. *Chem. Commun.* **2008**, 655. (e) Lulinski, S.; Zajac, K. *J. Org. Chem.* **2008**, *73*, 7785. (f) Slocum, D. W.; Reece, T. L.; Sandlin, R. D.; Reinscheld, T. K.; Whitley, P. E. *Tetrahedron Lett.* **2009**, *50*, 1593. (g) Lygin, A. V.; de Meijere, A. *Org. Lett.* **2009**, *11*, 389. (h) Cho, I.; Meimetis, L.; Britton, R. *Org. Lett.* **2009**, *11*, 1903. (i) Gupta, L.; Hoepker, A. C.; Singh, K. J.; Collum, D. B. *J. Org. Chem.* **2009**, *74*, 2231. (j) James, C. A.; Coelho, A. L.; Gevaert, M.; Forgiione, P.; Snieckus, V. *J. Org. Chem.* **2009**, *74*, 4094. (k) Narasimhan, S. K.; Kerwood, D. J.; Wu, L.; Li, J.; Lombardi, R.; Freedman, T. B.; Luk, Y.-Y. *J. Org. Chem.* **2009**, *74*, 7023.

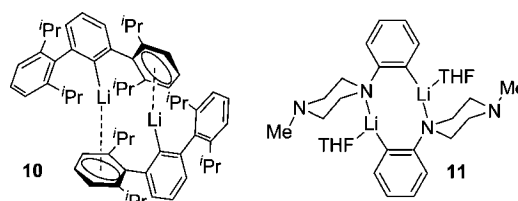
synthon for the preparation of a variety of metal complexes **4** via transmetalation reactions.⁴

The wide synthetic applications shown by *ortho*-lithiated species have fuelled intensive investigations toward elucidating their structures as a rational approach to understanding their reactivity.⁵ The results of these studies allow drawing a general picture about the preferred structures that *ortho*-lithiated compound may adopt. In the absence of strongly coordinating reagents, they tend to form aggregates by assembling monomeric units through electron-deficient C–Li–C bridges. In the most common aggregation state, the dimer, this binding mode leads to characteristics Li₂C₂ cores in which the deprotonated carbon is bound to two lithium atoms and the lithiums attain the favorite 4-fold coordination by chelation with the *ortho* functional group and/or through bonding to solvent molecules.⁵ *Ortho*-lithiated phosphazene **5**,⁶ carboxamides **6**⁷ and **7**,⁸ and oxazolidines **8**⁹ and **9**¹⁰ are representative examples of this self-aggregation mode (Scheme 2).

Scheme 2. Examples of *Ortho*-Lithiated Dimers



Scheme 3. Solid-State Structures of Aryllithium Dimers **10** and **11**



Aryllithiums devoid of polar substituents also dimerize by forming Li–C–Li–C four-membered rings.^{3a,4a,5c,j,11} Deviations from this structural motif have been observed only in two cases. The solid-state structure of (2,2'',6,6''-tetraisopropyl-1,1':3',1''-terphenyl-2'-yl)lithium (**10**) consists of a dimer in which the organic groups are linked through two Li⁺ ions showing η¹ and η⁶ C–Li bonds (Scheme 3).¹² Most probably, steric hindrance prevents the appropriate arrangement of monomers to give the usual C–Li–C bridges. In the phenyllithium derivative **11** dimerization involves rather uncommon C–Li–N–C bridges.¹³ No solution behavior has been described for either **10** or **11**.

A variety of phosphorus-containing functional groups have been shown to act as efficient directors of *ortho* lithiations.^{6,14} However, structural studies of the lithiated species have been limited to the solid-state characterization of lithium phosphazene **5**.⁶ Solution NMR data for complex **5** were measured at room temperature, so that they do not allow for identifying the species present in solution due to rapid exchange processes on the NMR time scale. Recently, we have shown that the deprotonation of *N*-benzyl-*N*-methyl-*P,P*-diphenylphosphinic amide **12** with *s*-BuLi in THF at –90 °C leads to the formation of benzylic and *ortho* anions **13** (Scheme 4).¹⁵ The benzylic anions undergo

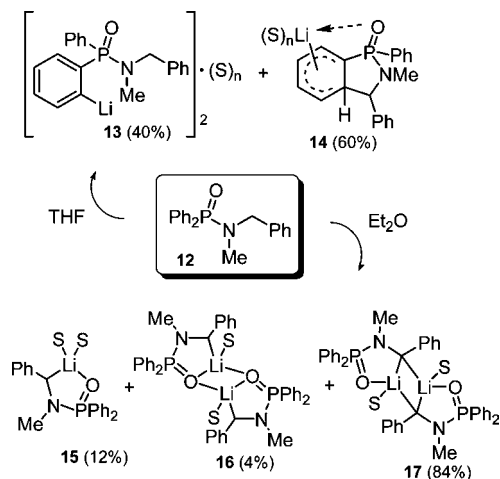
- (4) Selected references: (a) Kronenburg, C. M. P.; Amijs, C. H. M.; Jastrzebski, J. T. B. H.; Lutz, M.; Spek, A. L.; van Koten, G. *Organometallics* **2002**, *21*, 4662. (b) Baier, F.; Fei, Z.; Gornitzka, H.; Murso, A.; Neufeld, S.; Pfeiffer, M.; Rüdemaier, I.; Steiner, A.; Stey, T.; Stalke, D. *J. Organomet. Chem.* **2002**, *661*, 111. (c) Avent, A. G.; Hitchcock, P. B.; Leigh, G. J.; Togrou, M. *J. Organomet. Chem.* **2003**, *669*, 87. (d) Wei, P.; Chan, K. T. K.; Stephan, D. W. *Dalton Trans.* **2003**, 3804. (e) Koller, J.; Sarkar, S.; Abboud, K. A.; Veige, A. S. *Organometallics* **2007**, *26*, 5438. (f) Aguilar, D.; Contel, M.; Navarro, R.; Urriolabeitia, E. P. *Organometallics* **2007**, *26*, 4604. (g) Wu, C. J.; Lee, S. H.; Yu, S. T.; Na, S. J.; Yun, H.; Lee, B. Y. *Organometallics* **2008**, *27*, 3907. (h) Petrov, A. R.; Rufanov, K. A.; Harms, K.; Sundermeyer, J. *J. Organomet. Chem.* **2009**, *694*, 1212. (i) Barroso, S.; Cui, J.; Carretas, J. M.; Cruz, A.; Santos, I. C.; Duarte, M. T.; Telo, J. P.; Marques, N.; Martins, A. M. *Organometallics* **2009**, *28*, 3449. (j) Neshat, A.; Seambos, C. L.; Beck, J. F.; Schmidt, J. A. R. *Dalton Trans.* **2009**, 4987.
- (5) For recent references see: (a) Reich, H. J.; Goldenberg, W. S.; Sanders, A. W.; Tzschucke, C. C. *Org. Lett.* **2001**, *3*, 33. (b) Reich, H. J.; Goldenberg, W. S.; Gudmundsson, B. Ö.; Sanders, A. W.; Kulicke, K. J.; Simon, K.; Guzui, I. A. *J. Am. Chem. Soc.* **2001**, *123*, 8067. (c) Reich, H. J.; Goldenberg, W. S.; Sanders, A. W.; Jantzi, K. L.; Tzschucke, C. C. *J. Am. Chem. Soc.* **2003**, *125*, 3509. (d) Vestergren, M.; Eriksson, J.; Hilmersson, G.; Hakansson, M. *J. Organomet. Chem.* **2003**, *682*, 172. (e) Kronenburg, C. M. P.; Rijnberg, E.; Jastrzebski, J. T. B. H.; Kooijman, H.; Lutz, M.; Spek, A. L.; Gossage, R. A.; van Koten, G. *Chem.—Eur. J.* **2004**, *11*, 253. (f) Reich, H. J.; Goldenberg, W. S.; Sanders, A. W. *Arxivok* **2004**, *97*. (g) Kronenburg, C. M. P.; Rijnberg, E.; Jastrzebski, J. T. B. H.; Kooijman, H.; Spek, G. A. L.; van Koten, G. *Eur. J. Org. Chem.* **2004**, 153. (h) Arink, A. M.; Kronenburg, C. M. P.; Jastrzebski, J. T. B. H.; Lutz, M.; Spek, A. L.; Gossage, R. A.; van Koten, G. *J. Am. Chem. Soc.* **2004**, *126*, 16249. (i) Linnert, M.; Bruhn, C.; Rüffer, T.; Schmidt, H.; Steinborn, D. *Organometallics* **2004**, *23*, 3668. (j) Jantzi, K. L.; Puckett, C. L.; Guzei, I. A.; Reich, H. J. *J. Org. Chem.* **2005**, *70*, 7520. (k) Jambor, R.; Dostal, L.; Cisarova, I.; Rouzicka, A.; Holecek, J. *Inorg. Chim. Acta* **2005**, *358*, 2422. (l) Singh, K. J.; Collum, D. B. *J. Am. Chem. Soc.* **2006**, *128*, 13753. (m) Kawachi, A.; Tani, A.; Machida, K.; Yamamoto, Y. *Organometallics* **2007**, *26*, 4697. (n) Riggs, J. C.; Singh, K. J.; Yun, M.; Collum, D. B. *J. Am. Chem. Soc.* **2008**, *130*, 13709. (o) Chase, P. A.; Lutz, M.; Spek, A. L.; Gossage, R. A.; van Koten, G. *Dalton Trans.* **2008**, 5783. (p) Singh, K. J.; Hoepker, A. C.; Collum, D. B. *J. Am. Chem. Soc.* **2008**, *130*, 18008. (q) Konrad, T. M.; Gruenwald, K. R.; Belaj, F.; Moesch-Zanetti, N. C. *Inorg. Chem.* **2009**, *48*, 369. (r) Neshat, A.; Seambos, C. L.; Beck, J. F.; Schmidt, J. A. R. *Dalton Trans.* **2009**, 4987. (s) Petrov, A. R.; Rufanov, K. A.; Harms, K.; Sundermeyer, J. *J. Organomet. Chem.* **2009**, *694*, 1212.
- (6) Steiner, A.; Stalke, D. *Angew. Chem., Int. Ed. Engl.* **1995**, *34*, 1752.
- (7) Clayden, J.; Davies, R. P.; Hendy, M. A.; Snaith, R.; Wheatley, A. E. H. *Angew. Chem., Int. Ed.* **2001**, *40*, 1238.
- (8) Armstrong, D. R.; Boss, S. R.; Clayden, J.; Haigh, R.; Kirmani, B. A.; Linton, D. J.; Schooler, P.; Wheatley, A. E. H. *Angew. Chem., Int. Ed.* **2004**, *43*, 2135.
- (9) Stol, M.; Snelders, D. J. M.; Pater, J. J. M.; van Klink, G. P. M.; Kooijman, H.; Spek, A. L.; van Koten, G. *Organometallics* **2005**, *24*, 743.

(10) Jantzi, K. L.; Guzei, I. A.; Reich, H. J. *Organometallics* **2006**, *25*, 5390.

(11) (a) Ruhlandt-Senge, K.; Ellison, J. J.; Wehmschulte, R. J.; Pauer, F.; Power, P. P. *J. Am. Chem. Soc.* **1993**, *115*, 11353. (b) Dinnebie, R. E.; Behrens, U.; Olbrich, F. *J. Am. Chem. Soc.* **1998**, *120*, 1430. (c) Hino, S.; Olmstead, M. M.; Fettinger, J. C.; Power, P. P. *J. Organomet. Chem.* **2005**, *690*, 1638. (d) Strohmman, C.; Dilsky, S.; Strohmfeldt, K. *Organometallics* **2006**, *25*, 41. (e) Strohmman, C.; Gessner, V. H. *Chem.—Asian J.* **2008**, *3*, 1929.

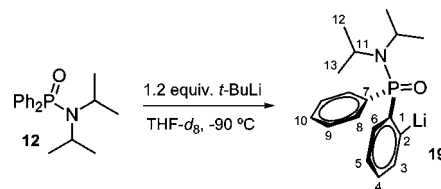
(12) Schiemenz, B.; Power, P. P. *Angew. Chem., Int. Ed. Engl.* **1996**, *35*, 2150.

(13) Spek, A. L.; Lakin, M. T.; Besten, R. Private communication, 1999; reference in Cambridge Structural Database: LEDQUG.

Scheme 4. Solution Structures of Lithium Benzyl, *Ortho*, and Dearomatized Phosphinic Amides Identified through NMR

anionic cyclization¹⁶ by attack to the *ortho* position of a *P*-phenyl ring, affording dearomatized species **14**.¹⁷ Benzylic and dearomatized lithium compounds were characterized as monomers, whereas the structure of *ortho* anions was tentatively assigned as dimers. Subsequent work from our group allowed us to devise reaction conditions suitable for the highly regioselective benzylic and *ortho* deprotonation of diphenylphosphinic amides. The former anions can be quantitatively generated in diethyl ether and have been used in carbon–carbon and carbon–heteroatom bond-forming reactions.¹⁸ Benzylic lithiation at $-90\text{ }^{\circ}\text{C}$ leads to a mixture of three anionic species, one monomer **15**, and two dimers showing Li_2O_2 , **16**, and Li_2C_2 rings, **17**, in a ratio of 12:4:84, respectively (Scheme 4).^{18a}

Ortho deprotonation is achieved in high yield by treating phosphinic amides devoid of acidic NC_α protons with *n*- or *t*-BuLi in THF at $-90\text{ }^{\circ}\text{C}$ (Scheme 4).¹⁹ Deprotonation of a *P*-phenyl ring of these substrates results in desymmetrized

Scheme 5. *Ortho* Lithiation of **18**

compounds, and we have begun to explore the applications of these ligands for developing new organometallic catalysts.²⁰ Very recently, we have achieved the process enantioselectively using the complex $[n\text{-BuLi}\cdot(-)\text{-sparteine}]$ as a source of chirality.²¹ The availability of one efficient procedure of phosphinic amide *ortho* lithiation allows for investigating the solution structures of these species. Here we report the results of the multinuclear magnetic resonance (^1H , ^7Li , ^{13}C , ^{31}P) study in THF solution and the computed structure using DFT methods of *ortho*-lithium *N,N*-diisopropyl-*P,P*-diphenylphosphinic amide **19**. At low temperature the anion exists as an equilibrium mixture of the monomer (ca. 17%) with two diastereomeric dimers (ca. 83%). The latter show a distinctive structural feature in aryllithium chemistry. In contrast to the C–Li–C bridges generally found in aggregated aryllithiums (see Scheme 2), monomers of **19** are self-assembled through O–Li bonds. To the best of our knowledge, this is the first time that dimerization of an aryllithium through formation of Li–O–Li–O four-membered rings has been characterized. Theoretical computations on model compounds of **19** indicate that dimers with the Li_2O_2 core are stabilized by $2.3\text{--}4.3\text{ kcal}\cdot\text{mol}^{-1}$, depending on the solvation degree, with respect to the alternative structural motif consisting of a Li–C–Li–C metallacycle. The analysis of the chemical bonding in Li_2C_2 and Li_2O_2 cores using the theory of atoms in molecules (AIM) showed that the Li_2O_2 ring is stabilized by a closed-shell interaction between the oxygen atoms, whereas the Li_2C_2 ring involves an unstable critical point connecting the carbon atoms. The calculated ^{13}C chemical shifts for monomers and dimers with different degrees of solvation strongly support the structures assigned in solution.

Results and Discussion

NMR samples were prepared in oven-dried 5 mm tubes by treating solutions of *N,N*-diisopropylidiphenylphosphinic amide **18** in THF- d_8 with 1.2 equiv of *t*-BuLi at $-90\text{ }^{\circ}\text{C}$ (Scheme 5; see Supporting Information for experimental details). Deprotonation of **18** leads to deep red solutions of $[\text{LiC}_6\text{H}_4\text{PhP}(\text{O})\text{N}(i\text{-Pr})_2]_2$ (**19**) that were transferred to the magnet previously cooled to the appropriate temperature.

Monitoring the species formed upon lithiation of organophosphorus compounds is best achieved through ^{31}P NMR spectroscopy.^{14m,15,18,22} The ^{31}P NMR spectra of **19** in the temperature range -110 to $0\text{ }^{\circ}\text{C}$ showed that lithiation was quantitative (less than 5% of unidentified species) and that no decomposition occurred (Figure 1). At $-60\text{ }^{\circ}\text{C}$ only a slightly broad singlet is observed at δ 38.12 ppm. This value represents a downfield shift of ca. 8 ppm relative to **18**, which suggests

- (14) Selected references: (a) Stuckwisch, C. G. *J. Org. Chem.* **1976**, *41*, 1173. (b) Dashan, L.; Trippett, S. *Tetrahedron Lett.* **1983**, *24*, 2039. (c) Yoshifuji, M.; Ishizuka, T.; Choi, Y. J.; Inamoto, N. *Tetrahedron Lett.* **1984**, *25*, 553. (d) Schaub, B.; Jenny, T.; Schlosser, M. *Tetrahedron Lett.* **1984**, *25*, 4097. (e) Craig, D. C.; Roberts, N. K.; Tanswell, J. L. *Aust. J. Chem.* **1990**, *43*, 1487. (f) Brown, J. M.; Woodward, S. *J. Org. Chem.* **1991**, *56*, 6803. (g) Gray, M.; Chapell, B. J.; Felding, J.; Taylor, N. J.; Snieckus, V. *Synlett* **1998**, 422. (h) López-Ortiz, F. *Curr. Org. Synth.* **2006**, *3*, 187. (i) Boubekeur, L.; Ricard, L.; Mézailles, N.; Demange, M.; Auffrant, A.; Le Floch, P. *Organometallics* **2006**, *25*, 3091. (j) Peveling, K.; Dannappel, K.; Schürmann, M.; Costisella, B.; Jurkschat, K. *Organometallics* **2006**, *25*, 368. (k) Tsuji, H.; Komatsu, S.; Kanda, Y.; Umehara, T.; Saeki, T.; Tamao, K. *Chem. Lett.* **2006**, *35*, 758. (l) Vinci, D.; Mateus, N.; Wu, X.; Hancock, F.; Steiner, A.; Xiao, J. *Org. Lett.* **2006**, *8*, 215. (m) García-López, J.; Fernández, I.; Serrano-Ruiz, M.; López-Ortiz, F. *Chem. Commun.* **2007**, 4674.
- (15) Fernández, I.; González, J.; López-Ortiz, F. *J. Am. Chem. Soc.* **2004**, *126*, 12551.
- (16) (a) Morán-Ramallal, A.; López-Ortiz, F.; González, J. *Org. Lett.* **2004**, *6*, 2141. (b) Ramallal, A.; Fernández, I.; López-Ortiz, F.; González, J. *Chem.—Eur. J.* **2005**, *11*, 3022.
- (17) (a) Review: López-Ortiz, F.; Iglesias, M. J.; Fernández, I.; Andújar-Sánchez, C. M.; Ruiz-Gómez, G. *Chem. Rev.* **2007**, *107*, 1580. See also: (b) Ruiz-Gómez, G.; Iglesias, M. J.; Serrano-Ruiz, M.; García-Granda, S.; Francesch, A.; López-Ortiz, F.; Cuevas, C. *J. Org. Chem.* **2007**, *72*, 3790. (c) Ruiz-Gómez, G.; Iglesias, M. J.; Serrano-Ruiz, M.; López-Ortiz, F. *J. Org. Chem.* **2007**, *72*, 9704. (d) López Ortiz, F.; Fernández, I.; Ruiz-Gómez, G.; Yañez-Rodríguez, V. (*PharmaMar S.A.*) PCT/WO2008/003809A1, 2008.
- (18) (a) Fernández, I.; López-Ortiz, F. *Chem. Commun.* **2004**, 1142. (b) Oña-Burgos, P.; Fernández, I.; Iglesias, M. J.; Torre-Fernández, L.; García-Granda, S.; López-Ortiz, F. *Org. Lett.* **2008**, *10*, 537.

- (19) Fernández, I.; Oña-Burgos, P.; Ruiz-Gómez, G.; Bled, C.; García-Granda, S.; López-Ortiz, F. *Synlett* **2007**, 611.
- (20) Oña-Burgos, P.; Fernández, I.; Rocas, L.; Torre-Fernández, L.; García-Granda, S.; López-Ortiz, F. *Organometallics* **2009**, *28*, 1739.
- (21) Popovici, C.; Oña-Burgos, P.; Fernández, I.; Rocas, L.; García-Granda, S.; Iglesias, M. J.; López-Ortiz, F. *Org. Lett.* **2010**, *12*, 428.

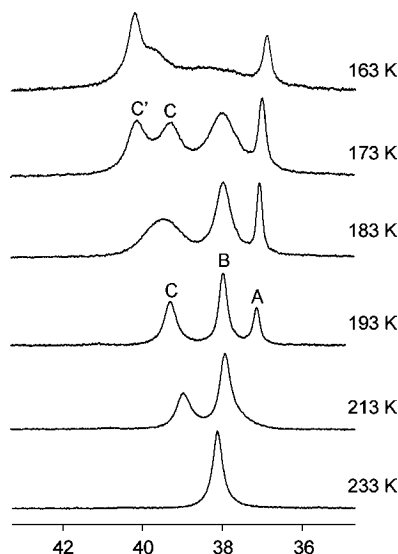


Figure 1. Variable-temperature ^{31}P (202.46 MHz) NMR spectra of 0.147 M **19** in $\text{THF-}d_8$.

that the $\text{P}=\text{O}$ group is coordinated to the lithium cation. At $-80\text{ }^\circ\text{C}$ this signal splits into three, **A** δ 37.2 ppm, **B** δ 38.0, and **C** δ 39.3 ppm. Decreasing the temperature to $-100\text{ }^\circ\text{C}$ produced a new splitting of **C** into two singlets: **C** (δ 40.2 ppm) and **C'** (δ 39.3 ppm), respectively. All signals except **A** are notably broad. At $-110\text{ }^\circ\text{C}$ the ^{31}P NMR spectrum is rather complicated probably due to conformational restrictions. Line broadening is expected for large molecules due to short transverse relaxation times, and therefore, if signals in the ^{31}P NMR spectra represent aggregates of different order (see below), the lowest degree would correspond to species **A**.

Ortho lithiation of **18** is readily ascertained from the ^1H NMR spectrum at $-60\text{ }^\circ\text{C}$. The deprotonated phenyl ring provides four multiplets in the aromatic region that were assigned through the analysis of their coupling pattern in the ^1H and $^1\text{H}\{^{31}\text{P}\}$ NMR spectra (Table 1).

Below $-60\text{ }^\circ\text{C}$ the proton spectra show the same features previously noted in the ^{31}P NMR spectra, and at the lowest temperature achieved a rather complicated spectrum with high signal overlapping is observed. In the ^{13}C and DEPT135 spectra at $-60\text{ }^\circ\text{C}$ the aromatic methine signals of the lithiated ring appear well spread at δ 141.18 (C3), 128.40 (C6), 125.23 (C4), and 120.64 (C5) ppm (Table 1). At this temperature the quaternary carbon signals are too broad and do not stand out from the noise of the spectrum. Interestingly, these chemical shifts are similar to those found for the corresponding carbons of lithiated phenyl derivatives in which the carbanion is bound to only one lithium ion (Figure 2).^{5c,10,23} Most importantly, the ^{13}C NMR spectrum measured at $-110\text{ }^\circ\text{C}$, a temperature where the exchange processes are slow on the chemical shift time scale,

Table 1. Selection of NMR Data (δ in ppm, J in Hz) of **19** Measured in $\text{THF-}d_8$ at $-60\text{ }^\circ\text{C}$

C/H	δ_{H}	$^nJ_{\text{PH}}$	δ_{C}	$^nJ_{\text{PC}}$
1			142.7 ^a	^b
2			209.2	^b
3	8.06	^b	141.2	31.7
4	6.86	2.1	125.2	4.7
5	6.78	7.2	120.6	14.4
6	7.52	7.8	128.4	25.7
7			137.3 ^a	^b
8	8.14	10.2	132.7	9.4
9	7.42–7.32	^b	127.4	11.5
10	7.42–7.32		130.0	
11	3.68	^b	47.3	2.3
12	1.23		23.1	2.7

^a Only observable via $^{13}\text{C}\{^{31}\text{P}\}$ NMR. ^b Not resolved.

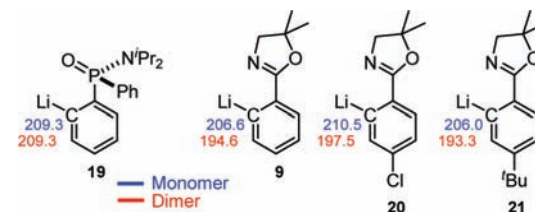


Figure 2. Comparison of ^{13}C Li chemical shifts of representative *ortho*-lithium compounds **9**, **20**, and **21** (data taken from ref 10) with **19**. Temperature of measurements is below $-100\text{ }^\circ\text{C}$ in all cases.

allows the identification of a broad multiplet at δ 209.3 ppm ($W_{1/2} = 162\text{ Hz}$) assigned to the carbon directly attached to the metal. Although the signal narrowed upon ^{31}P decoupling ($W_{1/2} = 107\text{ Hz}$), any possible coupling to ^7Li remained unresolved. Either the exchange rate is still rapid on the $^1J(^{13}\text{C}, ^7\text{Li})$ time scale or, most probably, the coupling is hidden by the overlap of several C–Li multiplets arising from the different species present in solution.

Although $^1J(^{13}\text{C}, ^7\text{Li})$ is lacking in **19**, the magnitude of the chemical shift strongly supports the existence of only one C–Li bond in the species existing in solution. Such a bonding situation is found in monomeric aryllithiums. It is well known that the aggregation state of aryllithiums can be correlated with the chemical shift of the *ipso* carbon. Increasing aggregation causes a shielding of the C_{ipso} due to the existence of a larger number of C–Li contacts.^{23,24} Thus, the C_{ipso} of $(\text{PhLi})_1$ and $(\text{PhLi})_2$ in THF at $-111\text{ }^\circ\text{C}$ appears at δ 196.4 and 188.2 ppm, respectively.^{5,23} Tetrameric PhLi in diethyl ether at $-106\text{ }^\circ\text{C}$ is characterized by a C_{ipso} carbon at δ 174.0 ppm.²³ Similar values are found for other *ortho* alkyl-substituted aryllithiums.^{5a–c,f,h} As expected, CLi carbons *ortho* to electron-withdrawing groups undergo deshielding as compared with PhLi. Dimers **5**, **8**, and **9** (Scheme 2) show in their ^{13}C NMR spectra lithiated carbons in the range δ 193.3–199.8 ppm. Monomers have been described only for **9** and some derivatives appropriately substituted at the carbon *para* to the oxazoline ring.¹⁰ In these compounds the C–Li carbon appears at δ 206.0–210.5 ppm (Figure 2). Additional deshielding is produced by lithium coordination to PMDTA or HMPA. A chemical shift difference larger than 12 ppm between CLi and C_2Li_2 binding modes allows an unequivocal assignment of monomeric and dimeric species. According to this analysis, the chemical shift of 209.3

- (22) (a) López-Ortiz, F.; Peláez-Arango, E.; Tejerina, B.; Pérez-Carreño, E.; García-Granda, S. *J. Am. Chem. Soc.* **1995**, *117*, 9972. (b) Fernández, I.; Álvarez-Gutiérrez, J. M.; Kocher, N.; Leusser, D.; Stalke, D.; González, J.; López-Ortiz, F. *J. Am. Chem. Soc.* **2002**, *124*, 15184. (c) Price, R. D.; Fernández, I.; Ruiz-Gómez, G.; López-Ortiz, F.; Davidson, M. G.; Cowan, J. A.; Howard, J. A. K. *Organometallics* **2004**, *23*, 5934. (d) Ruiz-Gómez, G.; Fernández, I.; López-Ortiz, F.; Price, R. D.; Davidson, M. G.; Mahon, M. F.; Howard, J. A. K. *Organometallics* **2007**, *26*, 514. (e) Fernández, I.; Davidson, M. G.; Price, R. D.; Lopez-Ortiz, F. *Dalton Trans.* **2009**, 2438.
- (23) Reich, H. J.; Green, D. P.; Medina, M. A.; Goldenberg, W. S.; Gudmundsson, B. Ö.; Dykstra, R. R.; Phillips, N. H. *J. Am. Chem. Soc.* **1998**, *120*, 7201.

- (24) (a) Seebach, D.; Hässig, R.; Gabriel, J. *Helv. Chim. Acta* **1983**, *66*, 308. (b) Bauer, W.; Winchester, W. R.; Schleyer, P. v. R. *Organometallics* **1987**, *6*, 2371. (c) Wehmschulte, R. J.; Power, P. P. *J. Am. Chem. Soc.* **1997**, *119*, 2847.

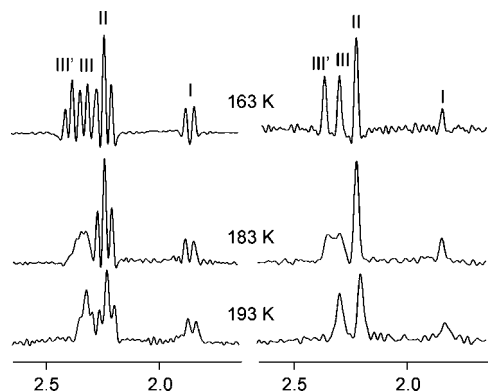


Figure 3. Variable-temperature ^7Li (left) and $^7\text{Li}\{^{31}\text{P}\}$ (right) NMR spectra (194.37 MHz) of 0.147 M **19** in $\text{THF-}d_8$. Species **III,III'** behave as a “fluxional ladder” at 193 K and a “static ladder” at 163 K (see text for explanations).

ppm for the lithiated carbon of **19** is consistent with a monomer or, strictly speaking, with an aggregation state where only one lithium–carbon bond exists.

The variable-temperature ^7Li NMR spectra provided the keys to unravel the solution structure of **19** (Figure 3). Analogously to the ^{31}P NMR spectra, decreasing the temperature from -60 to -80 °C transformed the singlet average signal at δ 2.12 ppm into three signals showing clearly resolved $^{31}\text{P}, ^7\text{Li}$ couplings: **I**, a doublet of $^{2/3}J(^{31}\text{P}, ^7\text{Li}) = 7.0$ Hz at δ 1.84 ppm, **II**, a triplet of $^{2/3}J(^{31}\text{P}, ^7\text{Li}) = 6.6$ Hz at δ 2.23 ppm, and **III**, a triplet of $^{2/3}J(^{31}\text{P}, ^7\text{Li}) = 4.8$ Hz at δ 2.33 ppm. At -110 °C **III** splits into two triplets **III** (δ 2.30 ppm, $^{2/3}J(^{31}\text{P}, ^7\text{Li}) = 6.5$ Hz) and **III'** (δ 2.37 ppm, $^{2/3}J(^{31}\text{P}, ^7\text{Li}) = 6.0$ Hz). The confirmation that the splitting of the signals does indeed proceed from the scalar coupling to ^{31}P was obtained through the acquisition of $^7\text{Li}\{^{31}\text{P}\}$ NMR spectra, where all multiplets collapsed into singlets.

We^{14m,15,18a,22} and others^{10,23,25} have previously shown the suitability of $J(^{31}\text{P}, ^67\text{Li})$ coupling constants for identifying the aggregation state of organolithium compounds. Lithium **I** is significantly shielded compared with **II** and **III** and shows the largest coupling constant with the phosphorus, two hints that clearly indicate a different aggregation state. The multiplicity of the lithium signals points out that Li(**I**) is coupled to only one phosphorus nucleus, whereas Li(**II**) and Li(**III**) are coupled to two phosphorus atoms. In all the concentration range assayed (see below), lithiums **III** and **III'** and phosphorus **C** and **C'** were always present in a ratio of 1:1, which suggests that both pairs of signals belong to the same species. The assignment of the ^{31}P and ^7Li NMR spectra was carried out through the 2D $^7\text{Li}, ^{31}\text{P}$ HMQC spectrum performed with ^1H decoupling during the whole sequence (Figure 4).^{18a} All possible correlations could

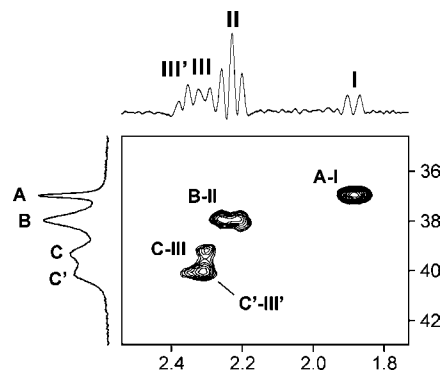


Figure 4. 2D $^7\text{Li}, ^{31}\text{P}\{^1\text{H}\}$ HMQC spectrum (194.37 MHz) of 0.147 M **19** at -100 °C in $\text{THF-}d_8$.

be detected, thus establishing the connectivity between the pairs **A-I**, **B-II**, and **C,C'-III,III'**.

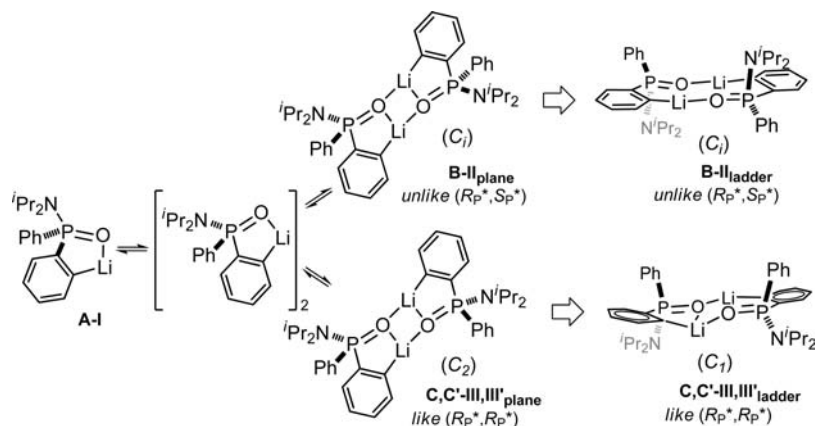
^{31}P NMR measurements in the concentration range 0.024–0.359 M revealed that the variations of the integrals of the ^{31}P signals **A** and **B,C** at -80 °C correlate reasonably well with an monomer–dimer equilibrium ($K_{\text{MD}} = 394 \text{ M}^{-1}$, Supporting Information) provided that the major species in the most diluted sample (0.024 M) is the monomer **A-I** (Scheme 6). Reasonably, in this monomer the oxygen atom would chelate the lithium, a feature supported by the deshielding of the ^{31}P nucleus as compared with the neutral phosphinic amide **18** (see above).

As aforementioned, the major lithium species present in solution ought to have only one C–Li bond. Therefore, dimerization cannot take place through the usual C_2Li_2 bridging of two monomers. In this arrangement the lithiated carbons would participate in three-center two-electron bonds. An alternative self-association mode of monomers that allowed us to explain the experimental results would consist of bridging the two organic fragments through the $\text{P}=\text{O}$ oxygen instead of the lithiated carbon (Scheme 6). Due to the chirality of **19**, this dimerization process might give rise to a mixture of two diastereoisomers corresponding to the *like* ($R_{\text{P}}^*, R_{\text{P}}^*$), **C,C'-III,III'**, and *unlike* ($R_{\text{P}}^*, S_{\text{P}}^*$), **B-II**, configurations. Dimers arranged in planar structures would lead to species with phosphorus and lithium atoms that are enantiotopic for **B-II**_{plane} (C_i symmetry) and homotopic for **C,C'-III,III'**_{plane} (C_2 symmetry). Therefore, the ^7Li and ^{31}P NMR spectra of these dimers would show only two signals. Things clarify if one considers that dimers exist in solution as fluxional ladder structures.^{26,27} Species **B-II**_{ladder} would retain its inversion center, contributing with one signal to the respective ^7Li and ^{31}P NMR spectra. However, **C,C'-III,III'**_{ladder} would show a time average signal for the lithium and phosphorus atoms above the coalescence temperature that would split in two when the dynamic process

(25) (a) Barr, D.; Clegg, W.; Mulvey, R. E.; Snaith, R. *J. Chem. Soc., Chem. Commun.* **1984**, 79. (b) Barr, D.; Doyle, M. J.; Mulvey, R. E.; Raithby, P. R.; Berd, D.; Snaith, R.; Wright, D. S. *J. Chem. Soc., Chem. Commun.* **1989**, 318. (c) Reich, H. J.; Green, D. P.; Phillips, N. H. *J. Am. Chem. Soc.* **1989**, *111*, 3444. (d) Reich, H. J.; Green, D. P. *J. Am. Chem. Soc.* **1989**, *111*, 8729. (e) Denmark, S. E.; Miller, P. C.; Wilson, S. R. *J. Am. Chem. Soc.* **1991**, *113*, 1468. (f) Reich, H. J.; Borst, J. P.; Dykstra, R. R.; Green, D. P. *J. Am. Chem. Soc.* **1993**, *115*, 8728. (g) Reich, H. J.; Kulicke, K. J. *J. Am. Chem. Soc.* **1996**, *118*, 273. (h) Reich, H. J.; Sikorski, W. H.; Gudmundsson, B. Ö.; Dykstra, R. R. *J. Am. Chem. Soc.* **1998**, *120*, 4035. (i) Reich, H. J.; Sikorski, W. H. *J. Org. Chem.* **1999**, *64*, 14. (j) Reich, H. J.; Holladay, J. E.; Walker, T. G.; Thompson, J. L. *J. Am. Chem. Soc.* **1999**, *121*, 9769. (k) Sikorski, W. H.; Reich, H. J. *J. Am. Chem. Soc.* **2001**, *123*, 6527.

(26) Fluxionality in ladder structures involving four-membered metallocycles has been used to describe intramolecular exchange/rearrangement processes. See for instance: (a) Clegg, W.; Greer, J. C.; Hayes, J. M.; Mair, F. S.; Nolan, P. M.; O'Neil, P. A. *Inorg. Chim. Acta* **1997**, 258, 1. (b) Primel, O.; Llauro, M.-F.; Pétaud, R.; Michel, A. *J. Organomet. Chem.* **1998**, 558, 19. (c) Arvidsson, P. I.; Ahlberg, P.; Hilmersson, G. *Chem.—Eur. J.* **1999**, *5*, 1348. The suggested fluxionality of complexes **B-II** and **C,C'-III,III'** represents the interconversion of different conformers; that is, no bond-breaking/bond-forming reactions take place. We thank one of the referees for directing our attention to this dynamic process.

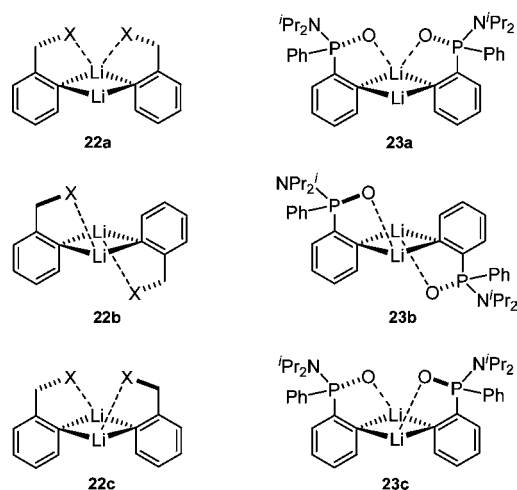
(27) The interconversion between conformers in ladder tetrameric $[(\text{PhLi})_4\{-(-)\text{-sparteine}\}_2]$ has been suggest to be slow on the NMR time scale. (a) Vestergren, M.; Eriksson, J.; Hilmersson, G.; Håkansson, M. *J. Organomet. Chem.* **2003**, 682, 172. (b) Sott, R.; Håkansson, M.; Hilmersson, G. *Organometallics* **2006**, *25*, 6047.

Scheme 6. Structures of the *Ortho*-Lithiated Compound **19** Present in THF Solution

is frozen out at 173–163 K due to the inequivalence of the monomeric fragments (C_1 symmetry). In this way, the “static” ladder structures would provide three ^7Li and ^{31}P NMR signals, as it is experimentally observed. Thus, **B-II_{ladder}** represents the *unlike* dimer and signals **C,C'-III,III'_{ladder}** correspond to the *like* aggregate, the ratio *like:unlike* being 0.8:1 (see computational studies and Figure S12). Puckered ladder structures involving three-coordinated lithium atoms in a distorted Li–O–Li–O core have been described in the solid state for chelated cyclopropenyllithium dimers.²⁸ Notwithstanding, one may assume that the lithium cations of all these species complete the preferred tetracoordination through binding to solvent molecules.²⁹ The line-broadening noticed in the ^1H NMR spectra at the lowest temperatures together with the somehow splitting of the ^{31}P signals of dimers **B** and **C** at temperatures below $-100\text{ }^\circ\text{C}$ is assigned to restricted rotation of the unsubstituted *P*-phenyl ring and/or the *N*-*i*-Pr₂ moiety, as has been mentioned before.³⁰ Interestingly, the Li–O–Li–O core found in dimers **B-II_{ladder}** and **C,C'-III,III'_{ladder}** is analogous to the self-association via O–Li bonds we have previously identified in dimers of NC α -lithiated phosphinic amides.^{18a} As far as we know, this is the first time that self-assembling of an *ortho*-aryllithium with formation of a Li–O–Li–O four-membered ring has been observed.

Amine and ether-chelated *ortho* aryllithiums have been shown to exist as an equilibrium mixture of dimeric isomers **22a**, **22b**, and **22c** (Scheme 7).^{5a–c,f,31} One might argue that lithium phosphinic amide **19** could behave similarly. The analogous structures **23a**, **23b**, and **23c** could lead to triplets in the ^7Li spectrum by assuming a fluxional behavior^{24a,29} in which rapid intramolecular exchange within the dimer would result in coupling of both lithiums to two phosphorus nuclei. However, structures **23a**, **23b**, and **23c** can be discarded on the basis of the ^{13}C chemical shift differences expected for CLi vs CLi₂ carbons noticed above.

Once the structure of the lithium species in solution was established, we decided to investigate the mechanism of

Scheme 7. Structures of Amine and Ether-Chelated Aryllithiums ($X = \text{NR}_2, \text{OR}$) and the Equivalent *Ortho* Lithium Phosphinic Amide **19**

equilibration among them.³² Exchange spectroscopy has become the method of choice to study multisite exchange and slow dynamic processes.^{33a} We measured a series of 2D phase-sensitive $^{31}\text{P}\{^1\text{H}\}$ EXSY spectra^{33b,c} with different mixing times τ_m to determine the way in which monomer **A-I** and dimers **B-II_{ladder}** and **C,C'-III,III'_{ladder}** are exchanging. At the lowest mixing time of 2.4 ms used (the instrumental limit) exchange is too slow to be detected and the spectrum showed only diagonal peaks (see Supporting Information). For $\tau_m = 50$ ms cross-peaks between both **B** and **C** with **A** are clearly observed (Figure 5). Increasing the mixing time to 100 ms favors the random exchange among all species in solution, although **B** and **C** are exchanging at a significantly lower rate, as deduced from the low intensity of the cross-peaks between them. These results indicate that dimers **B-II_{ladder}** and **C,C'-III,III'_{ladder}** exchange preferably through the monomer **A**; that is, they break up into

- (28) (a) Sorger, K.; Schleyer, P. V. R.; Stalke, D. *Chem. Commun.* **1995**, 2279. (b) Sorger, K.; Schleyer, P. V. R.; Fleischer, R.; Stalke, D. *J. Am. Chem. Soc.* **1996**, *118*, 6924.
- (29) (a) Bauer, W. P.; V. P.; Schleyer, P. V. P. *Adv. Carbanion Chem.* **1992**, *1*, 89. (b) Günther, H. In *Advanced Applications of NMR to Organometallic Chemistry*; Gielen, M., Willem, R., Wrackmeyer, B., Eds.; John Wiley: New York, 1996; Chapter 9, pp 247–290.
- (30) Restricted rotation of the P–C bond of phosphinic amides has been observed for the first time in dinaphthyl derivatives. Ruiz-Gómez, G. Ph.D. Thesis, Almería, 2006.
- (31) Reich, H. J.; Gudmundsson, B. Ö. *J. Am. Chem. Soc.* **1996**, *118*, 6074.

- (32) We would like to thank Prof. H. J. Reich for his helpful discussions and suggestions at the 8th International Symposium on Carbanion Chemistry (ISCC-8) held in Madison, WI, in 2008.
- (33) Reviews: (a) Perrin, C. L.; Dwyer, T. J. *Chem. Rev.* **1990**, *90*, 935. (b) Bain, A. D. *Prog. NMR Spectrosc.* **2003**, *43*, 63. See also: (c) Bircher, H.; Bender, B. R.; von Philipsborn, W. *Magn. Reson. Chem.* **1993**, *31*, 293. (d) Li, D. W.; Bose, R. N. *J. Chem. Soc., Dalton Trans.* **1994**, 3717. (e) Heise, J. D.; Raftery, D.; Breedlove, D. B. K.; Washington, J.; Kubiak, C. P. *Organometallics* **1998**, *17*, 4461. (f) Kesanli, B.; Charles, S.; Lam, Y.-F.; Bott, S. G.; Fettingner, J.; Eichhorn, B. *J. Am. Chem. Soc.* **2000**, *122*, 11101.

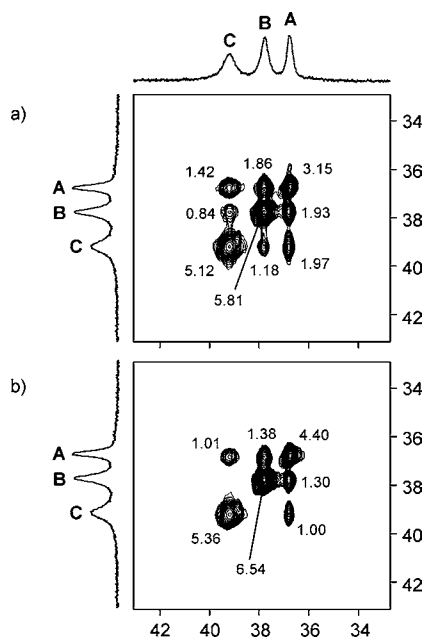


Figure 5. 2D $^{31}\text{P},^{31}\text{P}\{^1\text{H}\}$ EXSY NMR spectra (202.46 MHz) of 0.057 M **19** at -90°C in THF- d_8 with mixing times of (a) 100 ms and (b) 50 ms. The numbers shown on the 2D maps correspond to the relative cross-peak integrals.

monomers, which subsequently recombined back to dimers. The lack of cross-peaks between **B** and **C** at $\tau_m = 50$ ms validates this statement. The forward and reverse rate constants associated with the exchange process were calculated from the buildup of the cross-peak intensities of the 2D map, which are directly related to the exchange matrix.³⁴ At a mixing time of 50 ms the k_{-1} and k_1 between **A** and **B** are 4.5 and 5.9 s^{-1} . The corresponding rates of exchange between **A** and **C** are 4.6 and 4.1 s^{-1} , respectively.

Computational Study of 19. In order to understand the reasons for the observed self-aggregation of monomer **A-I** via O–Li bonds to give dimers **B-II_{ladder}** and **C,C'-III,III'_{ladder}**, instead of building up the Li_2C_2 core generally found in aryllithium dimers (Schemes 2 and 7), hybrid Hartree–Fock/density-functional theory computations at the B3LYP/6-311+G(2d,p) level were performed.³⁵ The degree of solvation of the lithium atoms was investigated too. The computations were carried out on model compounds in which the $N(i\text{-Pr})_2$ moiety of *ortho*-lithium phosphinic amide **19** was replaced by a NH_2 group. In the structures experimentally determined the amino substituents do not seem to be involved in any relevant interaction. Therefore, the model systems selected allow for simplifying the computational work without affecting the quality of the results. The calculated lithium species were labeled as **24M** and **24D**, where M and D stand for monomer and dimer, respectively. Differences in aggregation will be identified by adding to the name the specific Li_2O_2 or Li_2C_2 bridging mode contained in the structures. Analogously, solvation will be indicated by the number of THF molecules bound to lithium. Taking into account that dimers of *like* and *unlike* configuration are present in an almost 1:1 ratio in all NMR samples measured, geometry

Table 2. Energies (in atomic units) and Energy Differences (in $\text{kcal}\cdot\text{mol}^{-1}$) for the Species Studied in This Work^a

system	energy	ΔE
THF	−232.524645	
24M	−943.034946	0.0
24M·1THF	−1175.583334	−14.9 ^b
24M·2THF	−1408.119482	−22.1 ^b
24D-Li₂C₂	−1886.112993	−27.0 ^c
24D-Li₂O₂	−1886.119802	−4.3 ^d
24D-Li₂C₂·2THF	−2351.188559	−16.5 ^e
24D-Li₂O₂·2THF	−2351.192268	−2.3 ^f

^a Computations are at the B3LYP/6-311+G(2d,p) level of theory. ^b Relative to (**24M** + n THF), $n = 1$ or 2. ^c Relative to $2\times(\mathbf{24M})$. ^d Relative to **24D-Li₂C₂**. ^e Relative to $2\times(\mathbf{24M} + \text{THF})$. ^f Relative to (**24D-Li₂C₂** + 2THF).

optimizations of this type of aggregates were achieved only for structures of *unlike* relative configuration. The electronic DFT energies obtained are given in Table 2. Results indicate that dimer **24D-Li₂O₂** arising from self-assembling of **24M** through O–Li bonds is preferred to isomer **24D-Li₂C₂**, containing C–Li bridges, by 4.3 $\text{kcal}\cdot\text{mol}^{-1}$. On the basis that the lithium atom of organolithium compounds commonly adopts a tetracoordination either through aggregation or binding to donor solvent molecules,²⁹ we introduced the explicit solvent effect into our computations. Concerning energy, solvation by one molecule of THF of each lithium atom of dimers **24D** produced two effects. The THF-coordinated species are stabilized by an average amount of about 15 $\text{kcal}\cdot\text{mol}^{-1}$ relative to the solvent-free compounds, and the energy gap between **24D-Li₂O₂·2THF** and **24D-Li₂C₂·2THF** reduces to 2.3 $\text{kcal}\cdot\text{mol}^{-1}$. This means that both the unsolvated and THF-solvated dimer with the Li_2O_2 core are energetically favored as compared with the alternative aggregation through C–Li contacts to give dimers with the Li_2C_2 moiety, in full accordance with the NMR characterization. In addition, unsolvated **24M**, monosolvated **24M·1THF**, and disolvated **24M·2THF** were also optimized to ascertain the energy balance of aggregation (Figures S7, S8, and S9). Interestingly, the tricoordinated lithium of **24M·1THF** shows bond angles ranging from 96.9° to 148.5° . The largest value corresponds to the bond angle C(2)–Li–O(2) (Figure S8). Unusually large C–Li–O(THF) bond angles (range of 130 – 141.6°) in complexes having THF-solvated tricoordinated lithium atoms have been described in a number of cases.³⁶ Chelated aryllithium compounds show a strong tendency to aggregate,^{5a–c,f} and dimers **24D** provide further examples of this behavior. Unsolvated and THF-solvated dimers are stabilized with respect to the corresponding monomers (Table 2), thus explaining the thermodynamic preference experimentally observed for dimers (for instance, at a concentration 0.147 M in THF the ratio of monomer:dimers measured at -90°C is 83:17, Figure S5).

Dimers **24D-Li₂O₂** and **24D-Li₂C₂** present noticeably distinct structural characteristics (Figure 6). Compound **24D-Li₂O₂** is characterized by the participation of lithium in an essentially planar system (Figure 6b). Each monomeric unit acts as a C,O-chelating ligand of the lithium atom, affording a five-membered

(34) The free program EXSYCalc obtained from Mestrelab Research (<http://mestrelab.com/exsyncalc.html>) was employed.

(35) Frisch, M. J.; et al. *Gaussian 03*, Revision C.02; Gaussian, Inc.: Wallingford, CT, 2004. See Supporting Information for a complete list of authors.

(36) (a) Clark, D. L.; Gordon, J. C.; Huffman, J. C.; Watkin, J. G.; Zwick, B. D. *Organometallics* **1994**, *13*, 4266. (b) Wiberg, N.; Hwang-Park, H.-S.; Mikulcic, P.; Müller, G. *J. Organomet. Chem.* **1996**, *511*, 239. (c) Avent, A. G.; Bonafoux, D.; Eaborn, C.; Hill, M. S.; Hitchcock, P. B.; Smith, J. D. *J. Chem. Soc., Dalton Trans.* **2000**, 2183. (d) Asadi, A.; Avent, A. G.; Coles, M. P.; Eaborn, C.; Hitchcock, P. B.; Smith, J. D. *J. Organomet. Chem.* **2004**, *689*, 1238. (e) Forster, T. D.; Krahulic, K. E.; Tuononen, H. M.; McDonald, R.; Parvez, M.; Roesler, R. *Angew. Chem., Int. Ed.* **2006**, *45*, 6356.

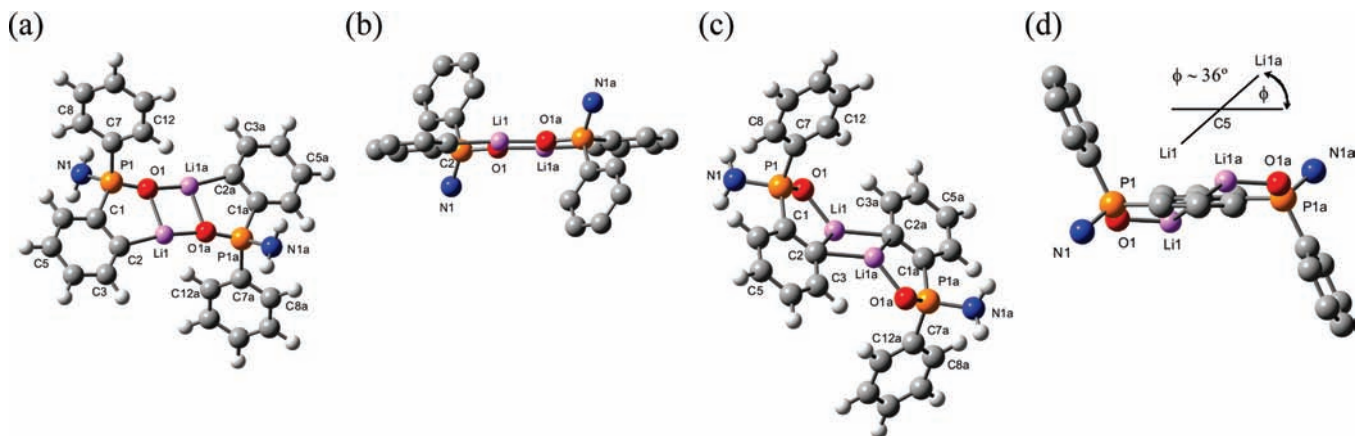


Figure 6. Top (a, c) and side-on views (b, d) of the DFT calculated (B3LYP/6-311+G(2d,p)) minimum energy structures of **24D-Li₂O₂** (a, b) along the C(2)–Li(1)–O(1a) plane and **24D-Li₂C₂** (c, d) along the C(5)–C(5a) axis. In (b) and (d) hydrogen atoms have been omitted for clarity. Twist angle in (d) is 36° (see text).

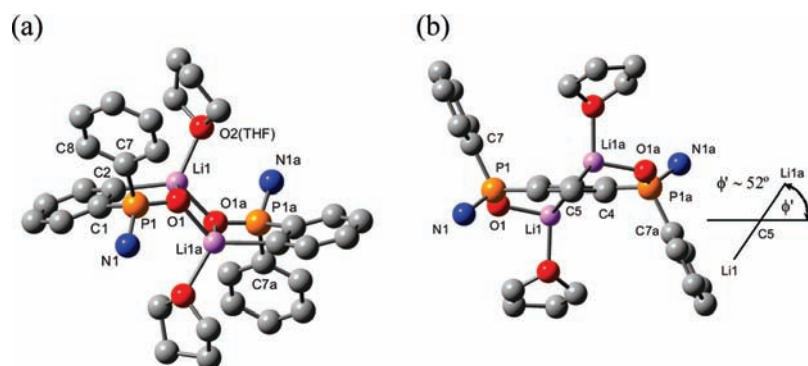


Figure 7. Side-on views of the DFT calculated (B3LYP/6-311+G(2d,p)) minimum energy structures of (a) **24D-Li₂O₂·2THF** and (b) **24D-Li₂C₂·2THF** (viewed along the C(5)–C(5a) axis). Hydrogen atoms have been omitted for clarity. Twist angle in (b) is 52° (see text).

metallacycle coplanar with the *ortho*-lithiated phenyl ring (torsion angle C(3)–C(2)–Li(1)–O(1) of -2.3°), and the Li(1)–O(1)–Li(1a)–O(1a) four-membered ring formed in the dimerization is completely planar. The deviation from planarity of the planes defined by the atoms O(1a)–Li(1)–O(1) and C(2)–Li(1)–O(1) is only 3.1° . In this arrangement, the phenyl rings of each monomeric fragment are too far apart (interproton distances larger than 5 Å) to generate any steric interaction. One might conclude that the structure of **24D-Li₂O₂** is in agreement with that proposed for **B-II_{ladder}** based on the NMR analysis. In contrast, **24D-Li₂C₂** shows a more compact structure (Figure 6c). The Li(1)–C(2)–Li(1a)–C(2a) four-membered ring has a rhomboid shape. The C(2)–Li(1) distance (2.238 Å) is 0.074 Å longer than the distance of C(2) to the lithium atom of the second monomer, Li(1a). This four-ring connects the two monomers to give a centrosymmetric structure in which the *ortho*-lithiated phenyl rings and the phosphorus atoms of the monomer units are coplanar, whereas one oxygen atom and the lithium atom coordinated to it lay above and beneath that plane (Figure 6d). Moreover, the lithium atoms are displaced from the perpendicular of the metalated phenyl ring. The twist angle between the Li(1)–C(2)–Li(1a) plane and the *ortho*-lithiated ring is ca. 36° . These features are similar to those found in the X-ray crystal structures reported for lithium-chelated **6**,⁷ **7**,⁸ **9**,¹⁰ and THF-solvated 2-(*N*-isopropyl-*N*-methyl)phenyllithium^{5b} and 1-(methoxy)-8-naphthyllithium.³⁷ The high degree of planarization shown by the CLi₂ carbon atoms is in agreement with

previous computational studies that predicted planar tetracoordinated carbons attached to two lithium atoms, R¹R²CLi₂, to be stabilized with respect to the tetrahedral geometry.³⁸ Chandrasekhar and Schleyer suggested that intramolecular chelation of lithium would increase the preference of the carbon atom for a planar arrangement.³⁹

Introducing solvation of each lithium atom by one molecule of THF produced a marked effect on the structure of dimer species with the Li₂O₂ core, **24D-Li₂O₂·2THF**. The tetracoordinated lithium atoms adopt a tetrahedral geometry (average sum of angles for lithium atoms of 338°) that converts the planar arrangement of **24D-Li₂O₂** into a ladder-type structure (Figure 7a). The “steps” consist of somewhat puckered monomers chelating each lithium atom (cf. torsion angles C(4)–C(3)–C(2)–Li(1) = 163.5° and C(6)–C(1)–P(1)–O(1) = 160.5°), which are connected through O–Li bonds, leading to a slightly distorted Li(1)–O(1)–Li(1a)–O(1a) four-membered ring (torsion angle of 3.1°). The *ortho*-metalated fragments are arranged centrosymmetrically around this ring at angles of ca. 126° (e.g., the angle between the O(1a)–Li(1)–O(1) and C(2)–Li(1)–O(1) planes is 124.7°). By contrast, **24D-Li₂C₂·2THF** retains the same structural characteristics of the unsolvated species. A very noticeable change induced by THF solvation is the increase of

(37) Betz, J.; Hampel, F.; Bauer, W. *Org. Lett.* **2000**, *2*, 3805.

(38) (a) Collins, J. B.; Dill, J. D.; Jemmis, E. D.; Apeloig, Y.; Schleyer, P. v. R.; Seeger, R.; Pople, J. A. *J. Am. Chem. Soc.* **1976**, *98*, 5419. (b) Sorger, K.; Schleyer, P. v. R. *J. Mol. Struct. (THEOCHEM)* **1995**, *338*, 317.

(39) Chandrasekhar, J.; Schleyer, P. v. R. *J. Chem. Soc., Chem. Commun.* **1981**, 260.

Table 3. Topological Properties of the Density at the Critical Points of the Four-Membered Rings of **24D-Li₂O₂** and **24D-Li₂C₂**^a

compd	bond	critical point	signature	$\rho_{\text{BCP}}(r)$	$\nabla^2\rho_{\text{BCP}}(r)$	λ
24D-Li₂O₂	O(1)–Li(1)	bond BCP(1)	(3, –1)	0.1718	4.2796	–0.983687, –0.880553, 6.143867
	O(1)–Li(1a)	bond BCP(2)	(3, –1)	0.2241	5.9316	–1.440513, –1.405110, 8.777396
	O(1)–O(1a)	bond BCP(3)	(3, –1)	0.0973	1.0124	–0.270036, –0.170598, 1.453064
	O(1)–Li(1a)–O(1a)	ring RCP(1)	(3, +1)	0.0917	1.3064	–0.297455, 0.473726, 1.130028
24D-Li₂C₂	C(2)–Li(1)	bond BCP(1)	(3, –1)	0.1623	2.4596	–0.759632, –0.675475, 3.894902
	C(2a)–Li(1)	bond BCP(2)	(3, –1)	0.1784	2.7972	–0.894755, –0.790312, 4.482386
	C(2)–C(2a)	bond BCP(3)	(3, –1) ^b	0.0887	0.3852	–0.217033, –0.001219, 0.603536
	C(2)–Li(1)–C(2a)	ring RCP(1)	(3, +1)	0.0887	0.3880	–0.217282, 0.002448, 0.603008

^a B3LYP/6-311+G(2d,p) computations. Density, Laplacian of the density, and eigenvalues of the Hessian of the density at the critical points in e/Å³, e/Å⁵, and e/Å⁵, respectively. ^b Note the almost vanishing second eigenvalue of the Hessian, hence very close to becoming a ring critical point (3,+1), as shown in the next row of the table and in Figure S11.

the twist angle between the Li(1)–C(2)–Li(1a) plane and the lithiated ring from 36° (no solvation) to 52° (Figure 7b). This is in fact an anticipated change. Increasing the number and/or strength of donor molecules intermolecularly bound to the lithium atoms of tetracoordinated CLi₂ carbons led to a larger deviation from planarity of the carbon geometry.³⁷ For instance, the twist angle in (1-(dimethylamino)-8-naphthyllithium·L)₂ of ca. 6° for L = Et₂O^{28b,40} increases to about 38° for L = THF.⁴¹

The Li₂C₂ core of **24D-Li₂C₂** determines that the *P*-phenyl substituent of one monomer unit is near the *ortho*-lithiated moiety of the other. The closest interproton distances are ca. 2.8 Å. These interatomic distances decrease to 2.6–2.7 Å in the THF-solvated species **24D-Li₂C₂·2THF**, i.e., below the threshold of 2.8 Å corresponding to the sum of van der Waals radii of two protons. This proximity effect might be a source of destabilization of dimers containing the Li₂C₂ core vs Li₂O₂ isomers. The calculated NBO charges do not show prominent differences, except for the lithium atom (Table S3). Its charge *q* (in units of |e|) increases in the series **24D-Li₂C₂** (*q*(Li) = 0.639) < **24D-Li₂O₂** (*q*(Li) = 0.706) < **24M** (*q*(Li) = 0.808). The calculated dipole moments for **24M**, **24D-Li₂C₂**, and **24D-Li₂O₂** are 2.78, 0, and 0 D, respectively, the two latter due to *C_i* symmetry (inversion). It seems that the steric effects present in dimers showing C–Li bridges disfavor this association mode. On the other hand, the loss of planarity in **24D-Li₂O₂** through lithium solvation appears to produce a destabilization of the system. While **24D-Li₂O₂** is stabilized by 4.3 kcal·mol^{–1} relative to **24D-Li₂C₂**, this energy difference reduces to 2.3 kcal·mol^{–1} for the corresponding THF-solvated species **24D-Li₂O₂·2THF** and **24D-Li₂C₂·2THF**.

In order to get insight into the larger stability of **24D-Li₂O₂/24D-Li₂O₂·2THF** with respect to **24D-Li₂C₂/24D-Li₂C₂·2THF**, we analyzed the electron density topology of the Li₂O₂ and Li₂C₂ cores in the respective dimers **24D-Li₂O₂** and **24D-Li₂C₂** using the AIM approach of Bader.⁴² The results are summarized in Table 3. The topological analysis of the electron density in the four-membered rings Li₂O₂ and Li₂C₂ shows that there are seven critical points in each case (see Figures S10 and S11 in the Supporting Information and Figure 8), which are reduced to four symmetry-unique critical points. The discussion follows along these four symmetry-unique critical points in the four-membered rings. There are three bond critical points: two bond critical points (BCP) along the Li–X (X = O, C) direction—BCP(1) and BCP(2) in Figures S10, S11, and 8—and a central bond critical point—BCP(3) in Figures S10, S11, and 8—located at the geometrical center of the four-membered ring Li₂X₂ (X = C, O). *The fourth critical point is a ring critical point—RCP(1) in Figures S10, S11, and 8—and is vital for the distinction of the electronic structure of both dimers. In Li₂O₂, both RCP(1)'s are relatively far away from the BCP(3) at the center, hence showing a clear O···O interaction in the ring (R_{OO} = 2.839 Å),⁴³ as shown by the different topological description of BCP(3) and RCP(1) and the electron density plus bond paths of the Li₂O₂ moiety displayed in Figure 8a.⁴⁴ The two triangles showing the RCP(1)'s are well apart from the central BCP(3), and there is a bond path joining the two oxygen atoms.*

- (40) (a) Jastrzebski, J. T. B. H.; van Koten, G.; Goubitz, K.; Arlen, C.; Pfeffer, M. *J. Organomet. Chem.* **1983**, *246*, C75. (b) Rietveld, M. H. P.; Wehman-Ooyevaar, I. C. M.; Kapteijn, G. M.; Grove, D. M.; Smeets, W. J. J.; Kooijman, H.; Spek, A. L.; van Koten, G. *Organometallics* **1994**, *13*, 3782.
- (41) Betz, J.; Hampel, F.; Bauer, W. *J. Chem. Soc., Dalton Trans.* **2001**, 1876.

(42) Bader, R. W. F. *Atoms in Molecules*; Oxford University Press: Oxford, 1994.

(43) (a) Bofill, J. M.; Olivella, S.; Solé, A.; Anglada, J. M. *J. Am. Chem. Soc.* **1999**, *121*, 1337. (b) Alkorta, I.; Elguero, J. *J. Chem. Phys.* **2002**, *117*, 6463. (c) Solimannejad, M.; Alkorta, I.; Elguero, J. *J. Chem. Phys. Lett.* **2009**, *474*, 253.

(44) Popelier, P. L. A. with a contribution from Bone, R. G. A. *MORPHY98*, a topological analysis program, 0.2 ed.; University of Manchester, Institute of Science and Technology: Manchester, England, 1999.

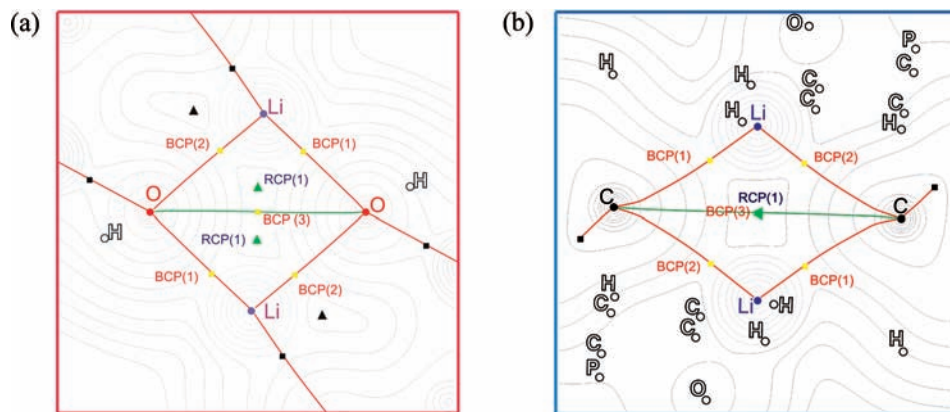


Figure 8. Bond paths and electron density for (a) the Li_2O_2 moiety in dimer **24D-Li₂O₂** and (b) the Li_2C_2 moiety in dimer **24D-Li₂C₂**. Filled squares and triangles correspond respectively to bond and ring critical points.

The positive sign of the Laplacian for all critical point indicates that the C–Li, O–Li, and O–O bonding interactions are characterized as closed-shell type. This is the expected kind of interaction for C–Li⁴⁵ and O–Li bonds.⁴⁶ Oxygen–oxygen closed-shell bonding interactions are not uncommon. They have been described, for example, for nitromethane,⁴⁷ $\text{Mn}_2(\text{CO})_{10}$ crystals,⁴⁸ biguanidinium dinitramide⁴⁹ and biguanidinium bis-dinitramide,⁵⁰ explosives such as pentaerythritol tetranitrate crystals,⁵¹ and open conformers of enols of *cis*- β -diketones⁵² and in the adsorption of nitro compounds on phyllosilicates.⁵³ O–O closed-shell and shared interactions have been found in silicates.⁵⁴ Bonding interactions between oxygen atoms seem to be unprecedented in organolithium compounds.

As regards to Li_2C_2 , the topological properties of BCP(3) at the center and RCP(1) are almost indistinguishable, hence an indication of the possibility of a near catastrophe point description of the electron density.^{43,55} There also appears a very weak C \cdots C interaction ($R_{\text{CC}} = 3.764 \text{ \AA}$), as deduced from the small magnitude of the Laplacian at the bond critical point linking C2 and C2a.⁵⁵ On the contrary, despite the short Li–Li distance

of 2.28 \AA , no bond critical point has been found between the metals. This is a structural feature previously encountered in the AIM analysis of other organolithium compounds.^{45,56} The bond paths and electron density for the Li_2C_2 moiety are displayed in Figure 8b, where both triangles representing the RCP(1)'s inside the four-membered ring and the central BCP(3) are practically located at the same point in space: the geometrical center of the Li_2C_2 ring. The almost vanishing second eigenvalue of the Hessian matrix in BCP(3) and RCP(1) for Li_2C_2 validates the above description. The existence of a catastrophe point is supported by the curvature of the bond paths connecting the carbon and lithium atoms. Since a change in structure implies that the system passes through a catastrophe point,⁵⁷ complex **24D-Li₂C₂** may be envisaged as an intermediate species along a reaction pathway in which two monomers **24M** self-assemble to give dimer **24D-Li₂O₂**, the thermodynamically most stable product.

The local stabilization provided by the O–O bonding interaction in **24D-Li₂O₂** together with the catastrophe point and the steric interactions found for the Li_2C_2 core of **24D-Li₂C₂** are the distinctive features that explain the preference of self-association of monomers of *ortho*-lithiated phosphinic amides through O–Li bonds, in agreement with the experimental results.

Taking into account that the ¹³C chemical shift of the lithiated *ipso*-carbon of **19** was crucial in the assignment of the structures in solution, we applied the DFT methodology to calculate the ¹³C chemical shifts of the model species **24** seeking to further support the structures experimentally determined. Of particular interest is the issue of solvation for which the NMR data proved to be inconclusive. Isotropic shifts were computed at the B3LYP/6-311+G(2d,p)//B3LYP/6-311+G(2d,p)/GAO level of theory⁵⁸ and converted to chemical shifts using TMS as standard. The calculated chemical shifts of the C_{*ipso*} carbons of unsolvated and THF-solvated monomers and dimers of **24** are displayed in Table 4. As aforementioned, it is well established the existence of a correlation between the magnitude of $\delta(^{13}\text{C})$ of lithiated carbons and the aggregation state.^{23,24} Recently, computational studies by Hilmersson et al. at the same level of theory used here have shown that the ¹³C chemical shift of the *ipso*-carbon

- (45) (a) Ritchie, J. P.; Bachrach, S. M. *J. Am. Chem. Soc.* **1987**, *109*, 5909. (b) Ponec, R.; Roithová, J.; Gironés, X.; Lain, L.; Torre, A.; Bochicchio, R. *J. Phys. Chem. A* **2002**, *106*, 1019. (c) Matito, E.; Poater, J.; Bickelhaupt, F. M.; Solà, M. *J. Phys. Chem. B* **2006**, *110*, 7189.
- (46) (a) Wang, Y.; Balbuena, P. B. *J. Phys. Chem. A* **2002**, *106*, 9582. (b) Gibbs, G. V.; Cox, D. F.; Crawford, T. D.; Rosso, K. M.; Ross, N. L.; Downs, R. T. *J. Chem. Phys.* **2006**, *124*, 084704/1. (c) Khartabil, H. K.; Martins-Costa, M. T. C.; Gros, P. C.; Fort, Y.; Ruiz-Lopez, M. F. *J. Phys. Chem. B* **2009**, *113*, 6459.
- (47) Cioslowski, J.; Mixon, S. T.; Fleischmann, E. D. *J. Am. Chem. Soc.* **1991**, *113*, 4751.
- (48) Bianchi, R.; Gervasio, G.; Marabello, D. *Inorg. Chem.* **2000**, *39*, 2360.
- (49) Zhurova, E. A.; Tsirelson, V. G.; Stash, A. I.; Pinkerton, A. A. *J. Am. Chem. Soc.* **2002**, *124*, 4574.
- (50) Zhurova, E. A.; Martin, A.; Pinkerton, A. A. *J. Am. Chem. Soc.* **2002**, *124*, 8741.
- (51) Zhurova, E. A.; Stash, A. I.; Tsirelson, V. G.; Zhurov, V.; Bartashevich, E. V.; Potemkin, V. A.; Pinkerton, A. A. *J. Am. Chem. Soc.* **2006**, *128*, 14728, and references therein.
- (52) Pakiari, A. H.; Eskandari, K. *J. Mol. Struct. (THEOCHEM)* **2007**, *806*, 1.
- (53) Muñoz-Santiburcio, D.; Ortega-Castro, J.; Sainz-Díaz, C. I.; Huertas, F. J.; Hernández-Laguna, A. *J. Mol. Struct. (THEOCHEM)* **2009**, *912*, 95.
- (54) Gibbs, G. V.; Downs, R. T.; Cox, D. F.; Ross, N. L.; Boisen, M. B., Jr.; Rosso, K. M. *J. Phys. Chem. A* **2008**, *112*, 3693.
- (55) (a) Oliva, J. M.; Allan, N. L.; Schleyer, P. v. R.; Viñas, C.; Teixidor, F. *J. Am. Chem. Soc.* **2005**, *127*, 13538. (b) Alkorta, I.; Blanco, F.; Elguero, J.; Dobado, J. A.; Melchor Ferrer, S.; Vidal, I. *J. Phys. Chem. A* **2009**, *113*, 8387.

- (56) Klobukowski, M.; Decker, S. A.; Lovallo, C. C.; Cavell, R. G. *J. Mol. Struct. (THEOCHEM)* **2001**, *536*, 189.
- (57) Bader, R. F.; Nguyen-Dang, T. T.; Tal, Y. *J. Chem. Phys.* **1979**, *70*, 4316.
- (58) Cheeseman, J. R.; Trucks, G. W.; Keith, T. A.; Frisch, M. J. *J. Chem. Phys.* **1996**, *104*, 5497.

Table 4. Computed SCF GIAO ^{13}C NMR Chemical Shifts ($\delta = \sigma_0 - \sigma$ ppm) of C_{ipso} Carbons in Model Compounds **24**^a

carbon	exptl ^b	24M	24M·1THF	24D-Li₂O₂	24D-Li₂C₂	24M·2THF	24D-Li₂O₂·2THF	24D-Li₂C₂·2THF
C(1)	142.7	149.2	149.3	146.3	149.8	150.4	145.5	150.2
C(2)	209.2	203.0	208.1	207.0	193.8	216.1	219.8	207.0
C(7)	137.4	141.9	143.6	140.7	143.2	144.9	143.9	143.9

^a Reference compound TMS: $\sigma(^{13}\text{C})_{\text{TMS}} = 183.4$ ppm. Computations at the B3LYP/6-311+G(2d,p) level of theory. ^b Measured in THF-*d*₈, -60 °C.

of PhLi is also sensitive to the solvation number at lithium.^{27b} The authors found that the computed value of $\delta(\text{C}_{\text{ipso}})$ of 177.3 ppm in unsolvated monomer (PhLi) increased to $\delta(\text{C}_{\text{ipso}})$ 183.6 and 193.2 ppm by lithium coordination to one and two molecules of Me₂O, respectively. Analogously, solvation of each lithium in (PhLi)₂ by one molecule of Me₂O produced a deshielding of the *ipso*-carbon from δ 175.4 ppm to δ 186.0 ppm ($\Delta\delta$ ca. 11 ppm). This chemical shift is almost identical to the $\delta(\text{C}_{\text{ipso}})$ reported for dimers of PhLi solvated by Et₂O (δ 188.0 ppm) and THF (δ 187.2 ppm).⁵⁹

The computed chemical shifts for the lithiated carbon of compounds **24** revealed that the experimental value of δ 209.2 ppm is in excellent agreement with those of monosolvated monomer **24M·1THF** (δ 208.1 ppm), unsolvated dimer **24D-Li₂O₂** (δ 207.0 ppm), and disolvated dimer **24D-Li₂C₂·2THF** (δ 207.0 ppm) (Table 2). The other *ipso*-carbons C(1) and C(7) of these species also show a good correlation between calculated and experimental ^{13}C chemical shifts. These results indicate that the computed chemical shifts of the C–Li carbons strongly support the preferred formation of lithium tricoordinated species, except for **24D-Li₂C₂·2THF**. The intriguing consequence of this study is that the NMR data seem to be equally consistent with dimers containing Li₂O₂ and Li₂C₂ cores, the subtle difference being the solvation degree of the lithium. Computational and experimental evidence allow for resolving this apparently structural uncertainty. The geometry optimization process showed that both unsolvated and THF-solvated compounds containing Li₂O₂ rings are stabilized with respect to the alternative Li₂C₂ dimers. In the same vein, the computed ^{13}C chemical shifts of the C–Li carbon in **24D-Li₂O₂** (δ 207.0 ppm) and **24D-Li₂C₂** (δ 193.8 ppm) are almost identical with those reported, respectively, for monomers and dimers of compounds **9**, **20**, and **21** in ethereal solvents (Figure 2). In our case, the monomer and dimer both appear at δ 209.2 ppm. This strongly supports the conclusion that **19** aggregates by forming Li–O–Li–O four-membered rings, leading to structures in which only one C–Li bond exists in each monomer unit. A corollary of this study is that, most probably, dimers **6**, **7**, **9**, **20**, and **21** reported in the literature¹⁰ exist in ethereal solutions as nonsolvated species. The coexistence of dimers with Li₂O₂ and Li₂C₂ arrangements in solution can be also discarded. Each self-assembling mode of racemic lithium phosphinic amide **19** would produce a pair of *like* and *unlike* diastereomeric species. Therefore, the ^{31}P and ^7Li NMR spectra of this mixture should exhibit an additional set of signals with respect to those experimentally detected for the existence of a single type of dimer.

The preceding analysis of ^{13}C chemical shifts of compounds **24** seems to disagree with the conclusions derived from the computed energies of these systems. The species predicted to prevail in solution on $\delta\text{C}_{\text{ipso}}$ grounds, **24M·1THF** and **24D-Li₂O₂**, bear a tricoordinated lithium and are thermodynamically disfavored relative to the tetracoordinated derivatives

24M·2THF and **24D-Li₂O₂·2THF**. The preference for the less solvated compounds may be due to entropic factors. Explicit coordination of a solvent molecule to a lithium atom entails an entropic cost. Therefore, if free energies rather than electronic energies are compared, it is possible that the lithium tricoordinated species become energetically favored.

To complete this section, we have extended the computational study to the structure of dimer **C,C'-III,III'**_{ladder}. The observation of unequivalent monomers in the ^7Li and ^{31}P NMR spectra has been explained through the lack of planarity of the ladder structure. With the aim of providing support to this statement, we have calculated the *in silico* structure of the “real” complex. We preferred to use the full molecule shown in Scheme 6 instead of the *like* isomer of the model dimer **24D-Li₂O₂-Li₂O₂** to avoid misleading subtle effects derived from the *syn* arrangement of the amino substituent bonded to phosphorus (hydrogen bonding, poor representation of steric interactions, etc.). Due to the size of the molecule, the calculations were performed at the B3LYP/6-31G* level of theory to achieve the computations within a reasonable period of time. The results are given in Figure S12 and Table S11 (Supporting Information). Frequency analysis confirmed that the computed structure is an energy minimum. The structure consists of two monomers slightly twisted with respect to each other, and this twist extends to the Li–O–Li–O four-membered ring connecting the subunits. These deviations from planarity originate a structure of *C*₁ symmetry that would represent the “static” ladder affording two signals in the ^7Li and ^{31}P NMR spectra measured at 163 K. Increasing the temperature accelerates the interconversion between conformers due to the flexibility of the system, and at 193 K only one average ^7Li and ^{31}P signal is observed.

Conclusions

In summary, we have achieved the structural characterization of an *ortho*-lithiated diphenylphosphinic amide for the first time. Multinuclear magnetic resonance (^1H , ^7Li , ^{13}C , ^{31}P) studies in THF under laboratory conditions, i.e., very low temperatures and natural abundance, showed that the anion exists as a mixture of one monomer and two diastereomeric dimers. The latter arise from *like* and *unlike* self-assembling of chiral monomers, leading to fluxional ladder structures. At 163 K the fluxional behavior of the *like* isomer is frozen out, breaking the equivalence of the two subentities in the dimer. We have demonstrated that dimerization takes place through oxygen–lithium bonds, leading to the formation of Li₂O₂ four-membered rings. This structural motif is unprecedented in aryllithium compounds, which generally self-assemble to give Li₂C₂ cores. Additional support for the structural assignment was provided by DFT computations on model compounds closely related to the real systems. The theoretical study evidenced that association of monomers via O–Li leads to dimers stabilized by 2.3–4.3 kcal·mol^{−1}, depending of the solvation degree, with respect to the alternative Li₂C₂ species. Bader analysis of the Li–C–Li–C and Li–O–Li–O four-membered rings allowed assigning the higher stability of the latter arrangement to the existence of a closed-

(59) (a) Hope, H.; Power, P. P. *J. Am. Chem. Soc.* **1983**, *105*, 5320. (b) Olmstead, M. M.; Power, P. P. *J. Am. Chem. Soc.* **1990**, *112*, 8008.

shell oxygen–oxygen bonding interaction, whereas the curved bond paths found in the Li_2C_2 core suggest that the corresponding dimer may represent a transient species in the pathway, leading to dimers Li_2O_2 . In addition, dimers containing the Li_2C_2 moiety are also destabilized by steric interactions. Importantly, the computed ^{13}C chemical shifts of the lithiated carbons of model C_2Li_2 and Li_2O_2 compounds support the existence of only one C–Li bond per monomer unit in dimers of *ortho*-lithiated **19**. The results obtained provide insight into the reactivity of *ortho*-lithium phosphinic amides.^{19,20} Further studies on enantiomerically pure derivatives are currently under progress.

Acknowledgment. Financial support by the Ministerio de Educación y Ciencia (MEC) (projects CTQ2005-1792BQU,

CTQ2008-117BQU, and MAT2009-14234-C03-02) and the Ramón y Cajal program (I.F.) is gratefully acknowledged. We thank Prof. F. Breher (Karlsruhe Institute of Technology) for his guidance in the attempted X-ray studies of **19** and Junta de Andalucía for a traveling grant. We are indebted to Prof. Ibon Alkorta for computing the bond paths from Figure 8a,b.

Supporting Information Available: Experimental details, 1D and 2D NMR spectra, as well as Cartesian coordinates and energies of the stationary points located. This information is available free of charge via the Internet at <http://pubs.acs.org>.

JA910556A